LIMNOLOGY AND OCEANOGRAPHY
Letters

ASLO
Open Access

Limnology and Oceanography Letters 2019
© 2019 The Authors. *Limnology and Oceanography* published by Wiley Periodicals, Inc. on behalf of Association for the Sciences of Limnology and Oceanography.
doi: 10.1002/lol2.10115

LETTER

Emergent productivity regimes of river networks

Lauren E. Koenig [1]*, *Ashley M. Helton* [1,2], *Philip Savoy* [3], *Enrico Bertuzzo* [4], *James B. Heffernan* [5], *Robert O. Hall Jr.* [6], *Emily S. Bernhardt* [3]

[1]Department of Natural Resources and the Environment, University of Connecticut, Storrs, Connecticut; [2]Center for Environmental Sciences and Engineering, University of Connecticut, Storrs, Connecticut; [3]Department of Biology, Duke University, Durham, North Carolina; [4]Department of Environmental Sciences, Informatics and Statistics, University of Venice Ca' Foscari, Venice, Italy; [5]Nicholas School of the Environment, Duke University, Durham, North Carolina; [6]Flathead Lake Biological Station, University of Montana, Polson, Montana

Scientific Significance Statement

The production of organic carbon by aquatic photosynthesis is a central ecosystem property that influences food webs and nutrient cycling rates. Although it is well known that several factors are related to variation in gross primary production in rivers, it is not known how these factors combine to determine primary productivity at the scale of river networks. Our simulation of river networks at a range of productivity regimes provides an initial approximation of river ecosystem productivity at broad scales, and shows that in some cases, small streams and certain time periods disproportionately influence river network productivity.

Abstract

High-resolution data are improving our ability to resolve temporal patterns and controls on river productivity, but we still know little about the emergent patterns of primary production at river-network scales. Here, we estimate daily and annual river-network gross primary production (GPP) by applying characteristic temporal patterns of GPP (i.e., regimes) representing distinct river functional types to simulated river networks. A defined envelope of possible productivity regimes emerges at the network-scale, but the amount and timing of network GPP can vary widely within this range depending on watershed size, productivity in larger rivers, and reach-scale variation in light within headwater streams. Larger rivers become more influential on network-scale GPP as watershed size increases, but small streams with relatively low productivity disproportionately influence network GPP due to their large collective surface area. Our initial predictions of network-scale productivity provide mechanistic understanding of the factors that shape aquatic ecosystem function at broad scales.

*Correspondence: lauren.koenig@uconn.edu

Author Contribution Statement: L.E.K., A.M.H., R.O.H., J.B.H., and E.S.B. conceived of the research question, and L.E.K. and A.M.H. designed the study. E.B. developed the simulated river networks, and L.E.K. performed the network-scale productivity analysis. All authors contributed to the interpretation and presentation of findings. L.E.K. wrote the paper with input from all authors.

Data Availability Statement: River productivity data and metadata are available in a CUAHSI Hydroshare repository (https://doi.org/10.4211/hs.eba152073b4046178d1a2ffe9a897ebe).

Associate editor: Alberto Borges

Additional Supporting Information may be found in the online version of this article.

This is an open access article under the terms of the Creative Commons Attribution License, which permits use, distribution and reproduction in any medium, provided the original work is properly cited.

At the scale of river networks, the seasonal dynamics of primary productivity determine the amount and timing of energetic inputs that feed mobile organisms and generate the export of labile carbon downstream. Understanding the characteristic patterns and controls on annual, network-scale productivity is therefore important to addressing fundamental questions in aquatic ecology because of the implications for food webs, nutrient cycling, and regional carbon budgets. However, current approaches primarily address the behavior of individual stream reaches over timescales spanning days to seasons, and limited empirical estimates of primary production throughout river networks (e.g., Rodríguez-Castillo et al. 2018; Saunders et al. 2018) constrain our ability to broadly predict patterns in network-scale productivity.

Within a river reach, light, heat, and hydrologic disturbance limit gross primary production (GPP) (Uehlinger 2000; Roberts et al. 2007). All rivers share these same constraints on productivity, but their relative importance differs among rivers as temporal fluctuations in various physical, chemical, and biological drivers act individually or in concert to determine the productivity regime for a river, that is, its characteristic annual pattern in GPP (Bernhardt et al. 2018). Recent improvements in the methods for monitoring dissolved gases and modeling metabolic rates (Hall and Hotchkiss 2017) have increased the availability of time series capturing daily, seasonal, and annual variation in GPP. Such data sets highlight the tremendous variability in productivity observed both within and across streams (Bernhardt et al. 2018), yet also enable new opportunities to characterize temporal patterns in reach-scale processes and resolve underlying causes of heterogeneity. For example, a recent synthesis showed that annual patterns of GPP observed across rivers could be categorized into discrete classes of rivers that share similar productivity regimes (Savoy et al. 2019), suggesting the existence of quantifiably distinct river functional types driven by common sets of underlying controls.

Longitudinal change in physical and chemical driver variables is often used to conceptualize expected variation in GPP from headwater streams to large rivers (Vannote et al. 1980). Daily and annual rates of GPP generally do increase with river size (Bott et al. 1985; McTammany et al. 2003; Finlay 2011), although factors that alter light availability, including watershed land use, can obscure longitudinal structure in GPP (Finlay 2011). Seasonal patterns in GPP may also vary with network position; large rivers with open canopies exhibit summer peaks in productivity (Uehlinger 2006), whereas in small, forested streams, terrestrial phenology and frequent scouring floods limit GPP to a relatively narrow temporal window (Roberts et al. 2007). Expected downstream shifts in the magnitude and timing of GPP suggest that network-scale patterns in productivity would vary with watershed size. Beyond reach-scales, however, rivers are not linear entities. The scaling transition from stream reaches to river networks thus requires quantifying and conceptualizing the heterogeneity, connectivity, and asynchrony (sensu McCluney et al. 2014) among spatially distributed patches that combine to form dynamic river networks (Poole 2002; Fisher et al. 2004). Prior research has established that reach-scale productivity regimes can be classified into characteristic functional types. Such classifications enable representation of the spatial heterogeneity in river ecosystems, and provide a framework for scaling ecosystem processes to network-scales.

To explore how the variation in primary production within and among individual stream *reaches* can give rise to emergent *river network* productivity regimes, we scaled annual stream productivity regimes using simulated river networks. We used these networks to address our overarching research question: To what extent are there distinct productivity regimes for river networks? Specifically, we used a conceptual modeling framework to examine how the magnitude and timing of annual, river-network GPP varies with (1) watershed size, and (2) reach-scale variation in light. Our goal was to highlight how different expectations regarding the spatial and temporal structure of GPP in rivers define a range of network-scale productivity regimes.

Methods

Simulated river networks

We used optimal channel networks (OCNs) to analyze emergent patterns of network-scale primary productivity. OCNs are derived as a function of least energy dissipation and are particularly useful for river network studies because they share the same fractal properties observed in natural drainage networks (Rinaldo et al. 1992; Rodríguez-Iturbe and Rinaldo 2001). For this study, we generated one OCN (512 × 512 pixels) following the procedure of Rinaldo et al. (1992). Pixel size was assumed equal to 100 m × 100 m, and so our simulated network drained a catchment area of 2621 km^2. Within this network, we sampled replicate subcatchments around four values of upstream area (40, 160, 450, and 2600 km^2; Supporting Information Fig. S1, Table S1) to investigate how the magnitude and timing of network GPP varies with watershed size.

We assumed that pixels within the OCN form an active stream channel when their drainage area, a proxy for threshold-limited fluvial erosion, exceeds a minimum threshold of 50 pixels, or 0.5 km^2. The OCNs were represented as directed networks using the *igraph* package (Csardi and Nepusz 2006) in R (R Core Team 2018). We calculated the width (m) of each node, or stream reach, as $W = 0.0013A^{0.479}$, where A is drainage area (m^2), based on the hydraulic geometry of streams and rivers that make up the GPP classification data set described below (Leopold and Maddock 1953; Savoy et al. 2019).

Reach-scale productivity regimes

We based our analysis of river-network GPP on a classification of reach-scale productivity regimes observed across a set of 47 streams and rivers in the continental United States (upstream area, mean: 1282 km^2; range: 7–17,551 km^2). Savoy et al. (2019) identified four groups of streams with similar temporal patterns in GPP, which they described as "spring peak," "summer peak,"

"aseasonal," and "summer decline" (Supporting Information Fig. S2). Here, we simulated river-network GPP by applying the empirical GPP time series to individual stream reaches within an OCN. We therefore did not explicitly model individual drivers of GPP such as light, temperature, nutrient supply, hydrology, or the community composition of primary producers. Rather, we expect that each distinct GPP regime reflects a common set of environmental drivers in streams exhibiting a given pattern (Savoy et al. 2019). Factors mediating GPP are thus implicitly represented in our analysis through the reach-scale regime classification assignments.

Channel width best predicted regime classification among streams in the empirical data set (Savoy 2019), and so we used three approaches to assign individual stream reaches to a given GPP regime based on width: (1) *Productive rivers*, where smaller streams (defined as width < 9 m) were assigned the "spring peak" regime and larger streams (width > 9 m) were assigned the "summer peak" regime; (2) *Unproductive rivers*, where larger streams (width > 9 m) exhibit the "aseasonal" productivity regime due to factors such as high turbidity or frequent scouring floods that limit light availability and algal biomass accrual; and (3) *Stochastic* assignment, where the probability of being assigned to any of the four reach-scale productivity regimes varied with river width. Smaller streams were most likely to follow the "spring peak" regime and larger streams were most likely to follow the "summer peak" regime (Supporting Information Table S2). We propose that the *Stochastic* scenario is likely most representative of real river networks because it captures the local heterogeneity in GPP that is expected along rivers. However, the three approaches together serve to constrain the envelope of possible network-scale productivity regimes.

After assigning each stream reach to a regime based on the *Productive rivers*, *Unproductive rivers*, or *Stochastic* scenario, we randomly assigned each reach to a specific annual GPP time series from among those classified under that regime (Savoy 2019). Reach-scale areal productivity rates (g O_2 m^{-2} d^{-1}) were converted from O_2 to C units assuming a 1:1 molar relationship between carbon and oxygen, and then multiplied by streambed surface area (m^2) to calculate daily rates of GPP for each stream reach (g C d^{-1}). We quantified river-network GPP (kg C d^{-1}) by summing daily estimates of reach-scale GPP across the individual stream reaches that comprise the river network. We evaluated the timing of annual network productivity for each model scenario and watershed size by calculating the day of year that exceeded 50% of annual, network-scale GPP. We resampled the empirical time series and repeated network-scale simulations 1000 times. Confidence intervals were calculated from the 95% quantiles of the modeled distribution.

Modeled light availability scenarios

To explore how factors affecting light availability in streams—including the structure and phenology of riparian vegetation—might influence river-network productivity, we evaluated two additional model scenarios. First, we increased the length of the spring GPP peak, as might be expected given a longer lag between snowmelt and terrestrial leaf-out in temperate forests (Creed et al. 2015). We hypothesized that an extended vernal window, characterized by high incident light reaching streams combined with earlier onset of warmer water temperatures, leads to a corresponding increase in the duration of the spring GPP peak. Specifically, in this "vernal window" scenario, we modified the "spring peak" regime so that GPP begins to increase 7 d and 14 d earlier, respectively, although we assumed that peak GPP remains the same (Supporting Information Fig. S3a). We applied the modified productivity regimes to all stream reaches in the river network that were assigned the "spring peak" regime.

Implicit in the "spring peak" regime is that light constrains GPP for much of the year due to shading by the terrestrial canopy. In the "riparian clearing" scenario, we modified the reach-scale assignments to simulate river-network GPP under conditions where light does not limit GPP in small streams, for example, in a terrestrial biome with fewer trees, or due to riparian clearing. We hypothesized that in the absence of riparian forest, small streams would adopt a "summer peak" regime, where stream GPP is more closely aligned with temporal patterns in incoming light and the terrestrial growing season. Therefore, in this scenario, we randomly selected 20–100% of reaches originally characterized by the "spring peak" regime and reassigned them as "summer peak" streams to simulate removing canopy shading as a constraint on primary productivity over varying spatial extents. We applied the vernal window and riparian clearing scenarios to our simulated river network given each of the three baseline model scenarios (i.e., *Productive rivers*, *Unproductive rivers*, and *Stochastic*).

Results

River network productivity regimes

Simple scaling of the observed distribution of GPP across stream sizes yielded a wide range of potential river-network productivity regimes. For our simulated river network, network-scale GPP followed a somewhat bimodal pattern when large river segments were assumed to be relatively productive (Fig. 1a). Under this scenario, network-scale GPP was highest during the summer (day 207) when large river reaches were highly productive relative to small streams (Fig. 1d). In contrast, peak network productivity occurred earlier in the year for both the *Stochastic* (day 109; Fig. 1b) and the *Unproductive rivers* scenarios (day 95; Fig. 1c). In the *Unproductive rivers* scenario, the spring-time GPP peak was driven by metabolic activity in small streams (Fig. 1f), and 50% of annual network productivity was accumulated by day 158 (compared to day 183 for the *Productive rivers* scenario; Table 1). The *Stochastic* scenario differed from the two other modeled scenarios in that the spatial distribution of GPP at the time of peak network productivity was relatively uniform throughout the river network (Fig. 1e). Therefore, while a substantial proportion of annual, network

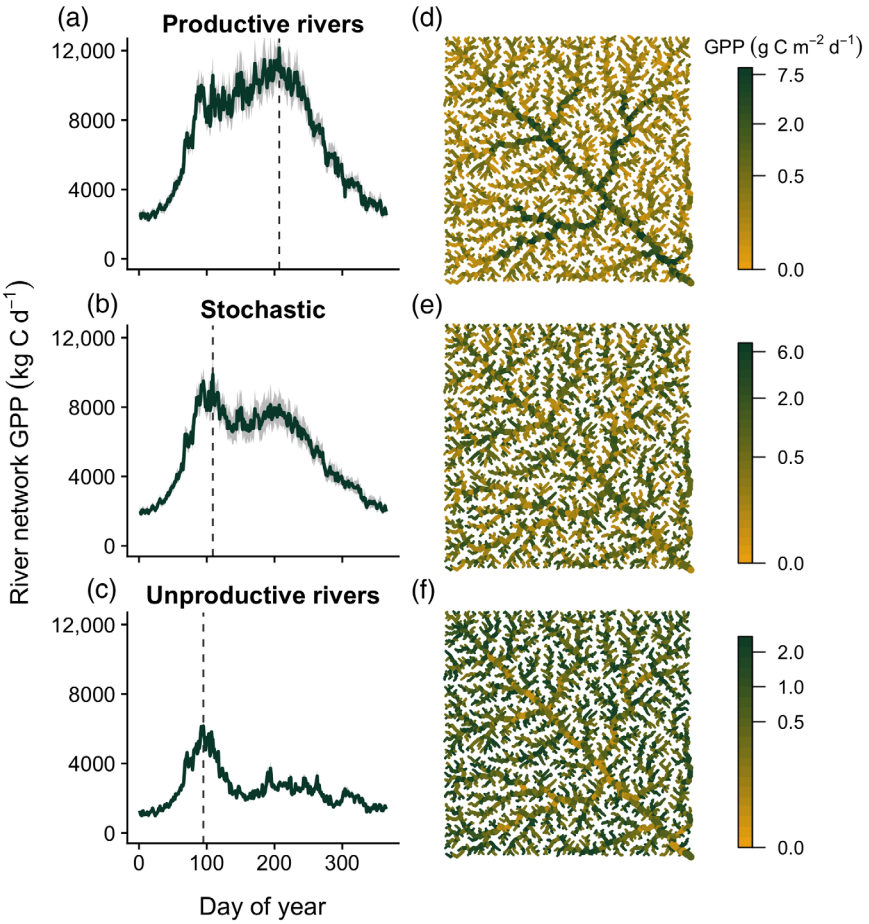

Fig. 1. The envelope of annual river-network productivity regimes for a 2621 km^2 watershed. The timing and magnitude of river-network GPP varies depending on whether (**a**) all large rivers are productive, (**b**) the probability of a reach following a given regime varies with stream width, or (**c**) all large rivers are unproductive. The spatial distribution of reach-scale GPP is shown for the day of maximum river-network productivity (dashed lines in panels **a**–**c**) for each of the (**d**) *Productive rivers*, (**e**) *Stochastic*, and (**f**) *Unproductive rivers* scenarios.

GPP is accumulated earlier in the year, spring-time productivity in the *Stochastic* scenario reflects the metabolism of both small streams and larger rivers.

Overall, the timing of peak productivity covaried with the magnitude of annual, network-scale GPP (Table 1). In small watersheds (e.g., 40 km^2), river network GPP is limited to a short period in the spring when incident light reaching headwater streams is high prior to terrestrial leaf-out. Small watersheds do not include river segments wide enough to be designated as large rivers under the *Productive rivers* and *Unproductive rivers* scenarios, so the network productivity regimes for these two scenarios were identical (Fig. 2; 40 km^2). However, assuming large rivers are productive, the distribution of network GPP shifted later in the year as watershed size increased and more large rivers were sampled (Fig. 2).

In intermediate-sized watersheds (e.g., 160 km^2), we observed substantial variability in the temporal pattern of network GPP for the *Productive rivers* scenario, where replicate subcatchments adopted either the spring-dominated pattern or the bimodal regime characteristic of larger watersheds (Fig. 2). For the *Productive rivers* and *Unproductive rivers* scenarios, the overall network pattern was sensitive to the number of river segments wider than 9 m, and therefore, to small differences in network shape (e.g., elongation) among subcatchments of equal size. Similarly, the network regime was variable among 40 km^2 subcatchments given stochastic assignment of reach-scale productivity regimes. In either case, as watershed size increases, heterogeneity among reaches is averaged out at the network-scale.

Across a range in watershed size, annual, network-scale GPP increased disproportionately relative to drainage area (i.e., allometric scaling with exponent > 1; Supporting Information Fig. S4), especially for the *Productive rivers* scenario, where mean areal productivity rates were greater in larger watersheds (Table 1). The shape and magnitude of the network-scale productivity regime changes as watershed size increases and cumulative, river-network GPP captures the metabolic activity of larger river reaches. However, a substantial proportion of

Table 1. The magnitude and timing of river network GPP varies with watershed size. Values indicate the mean and standard deviation (in parentheses) across 1000 realizations of sampling reach-scale productivity regimes and across replicate subcatchments within our simulated network (Supporting Information Fig. S1): 40 km^2 (n = 13), 160 km^2 (n = 5), 450 km^2 (n = 2), and 2600 km^2 (n = 1).

Watershed size (km^2)	Modeled scenario	Annual river network GPP (kg C yr^{-1})	Mean daily GPP (g C m^{-2} d^{-1})	Day of year, 50% annual GPP
40	Productive	8650 (1220)	0.29 (0.04)	117 (2.4)
	Stochastic	14,900 (3620)	0.49 (0.12)	157 (9.9)
	Unproductive	8660 (1210)	0.29 (0.04)	117 (2.3)
160	Productive	65,700 (14,200)	0.46 (0.09)	156 (11.8)
	Stochastic	66,800 (7980)	0.47 (0.05)	157 (3.8)
	Unproductive	40,700 (2930)	0.28 (0.02)	127 (5.0)
450	Productive	287,000 (31,100)	0.62 (0.06)	175 (2.6)
	Stochastic	233,000 (19,500)	0.50 (0.04)	160 (3.5)
	Unproductive	131,000 (4850)	0.28 (0.01)	140 (4.6)
2600	Productive	2,520,000 (121,000)	0.77 (0.04)	183 (0.8)
	Stochastic	1,960,000 (96,500)	0.60 (0.03)	173 (1.0)
	Unproductive	916,000 (15,300)	0.28 (0.01)	158 (2.8)

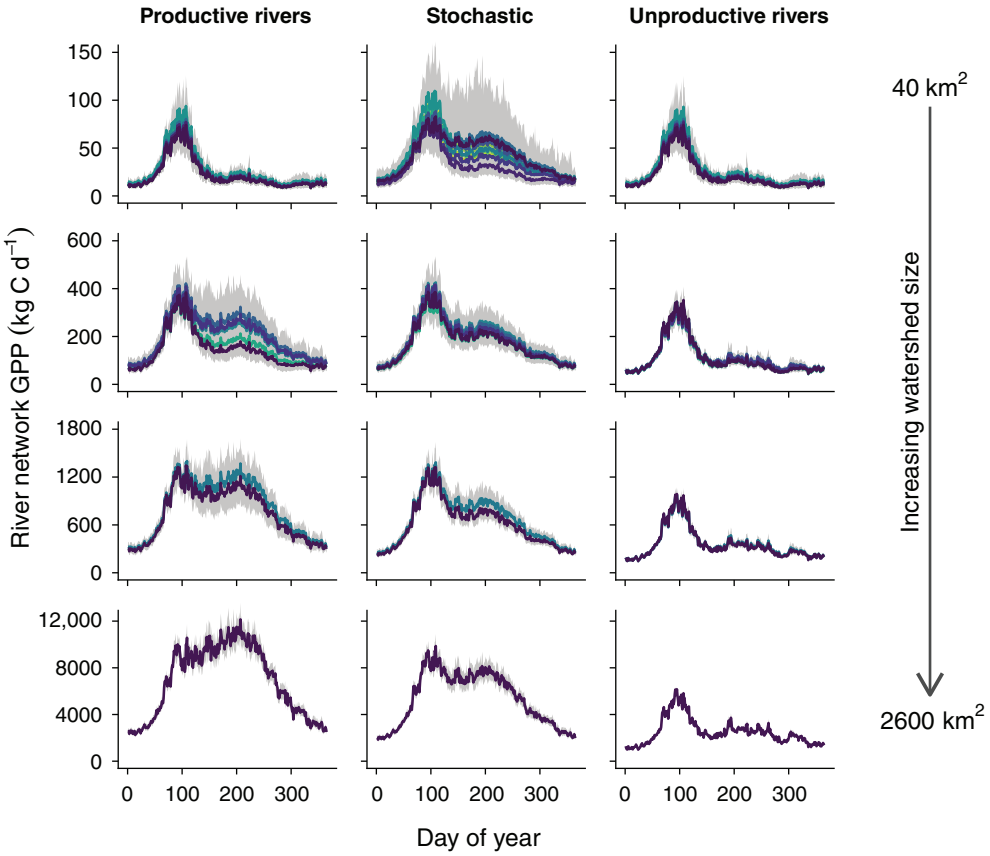

Fig. 2. Annual productivity regimes for catchments draining 40, 160, 450, and 2600 km^2 under three modeled productivity scenarios. Colored lines show the mean productivity regimes for different subcatchment size replicates (40 km^2: n = 13, 160 km^2: n = 5, 450 km^2: n = 2, and 2600 km^2: n = 1), and gray shading indicates the 95% confidence intervals. Annual, network-scale GPP is increasingly dominated by summer productivity in rivers for larger watersheds under the *Productive rivers* and *Stochastic* scenarios. In watersheds where larger rivers are relatively unproductive, spring GPP in headwater streams drives the annual regime.

annual, network-scale productivity is derived from small streams (Fig. 3), irrespective of watershed size. For example, streams draining 100 km^2 or less contributed 21% of annual GPP in our simulated network, given the *Productive rivers* scenario and 57% of annual GPP given the *Unproductive rivers* scenario. Despite their relatively low productivity on an individual basis, collectively, small streams constitute a large proportion of benthic surface area in river networks; stream segments draining 100 km^2 or less represent 56% of benthic surface in our 2621 km^2 network (Fig. 3). Therefore, their cumulative effect on river-network productivity is large.

Modeled light availability scenarios

Modifying reach-scale productivity regimes to implicitly increase light availability in small streams resulted in greater annual, network GPP relative to our baseline model scenarios. In our simulated network, extending the vernal window by as much as 14 d weakly increased annual, network-scale GPP by approximately 2%, 2%, and 5% for the *Productive rivers*, *Stochastic*, and *Unproductive rivers* scenarios, respectively (Supporting Information Table S3). Removing the light constraint from riparian vegetation in a subset of streams had a more appreciable effect on network-scale GPP. Relative to the baseline scenario, shifting 20% of small streams to the "summer peak" regime increased annual, network-scale GPP by 16%, 17%, and 44% for the *Productive rivers*, *Stochastic*, and *Unproductive rivers* scenarios, respectively (Supporting Information Table S3). Increasing the proportion of small streams without riparian shading resulted in a shift in the timing of peak productivity toward a summer-dominated regime at the network-scale (Fig. 4), suggesting that widespread riparian clearing adjacent to headwater streams has considerable effects on network-scale patterns of productivity.

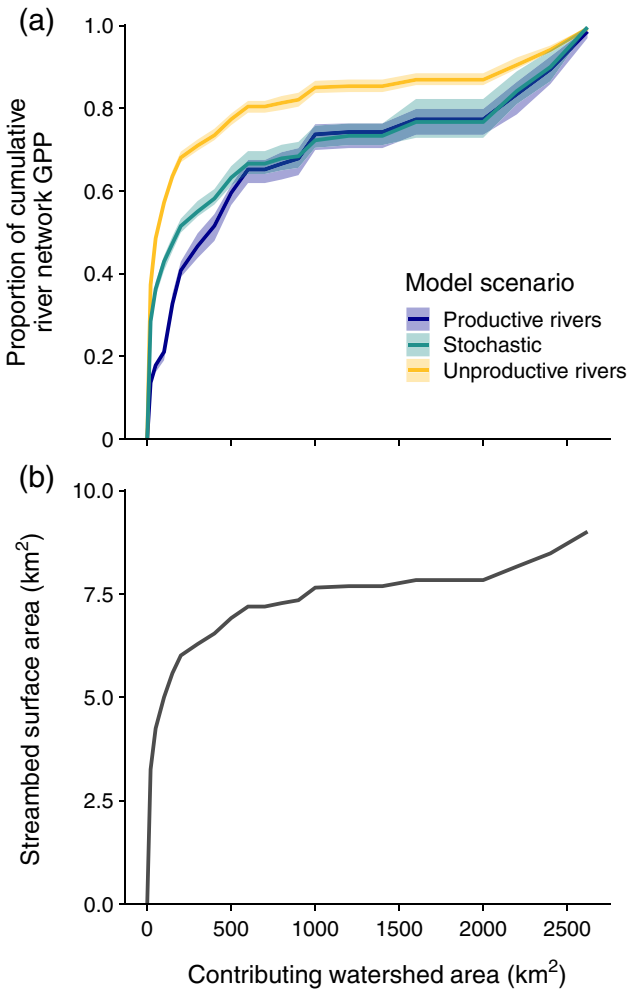

Fig. 3. Small streams contribute a substantial proportion of (**a**) river network GPP due to their (**b**) large cumulative streambed surface area. Mean estimates (± 95% confidence intervals) for the fraction of network-scale GPP represented by a given upstream drainage area are shown for a 2621 km^2 watershed.

Discussion

Using simulated river networks, we show that even simple assumptions about scaling empirical rates of GPP can yield a wide range of network productivity regimes that vary with watershed size, the productivity of large rivers, and the riparian light regime. Productivity in larger river segments became more influential on the magnitude and timing of network-scale GPP as watershed size increased, although small streams with relatively low productivity contributed a substantial proportion of annual, network GPP due to their large collective surface area. As a result, modeled shifts in the light regime in small streams substantially altered the magnitude and distribution of network-scale primary production. Together, these results suggest that network productivity regimes may be highly variable, but are also sensitive to factors affecting the amount or timing of GPP in small streams.

Our goal was to explore the envelope of river-network productivity regimes by deriving network-scale estimates of GPP for clear end-members of the likely distribution of productivity regimes in real networks. The large differences that emerge between these end-member scenarios generate initial hypotheses for how we should expect the magnitude and timing of network productivity to be structured as a function of the relative number and distribution of different stream ecosystem functional types (sensu Montgomery 1999). Our method for assigning reach-scale regimes in the *Productive rivers* and *Unproductive rivers* scenarios divides the population of river reaches into only two functional types depending on river width. These modeled scenarios therefore do not capture the local heterogeneity in light and GPP that is expected along a river continuum due to local variation in canopy cover, topography, and geomorphology (Julian et al. 2008*a*, *b*). For this reason, we expect that the *Stochastic* scenario, in which any given reach within the network can follow any of four empirical productivity regimes, is more likely to represent the behavior of real drainage networks, and may provide a reliable first approximation of GPP at broad scales.

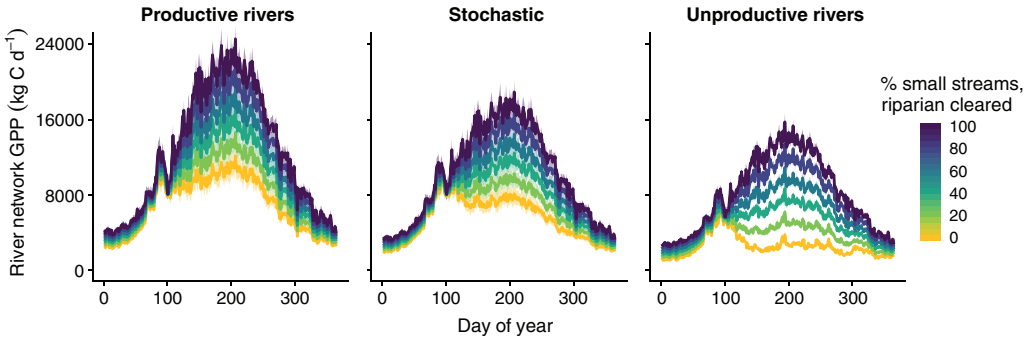

Fig. 4. Riparian clearing increases annual, river-network GPP and shifts the peak in network productivity toward the summer. Mean estimates (± 95% confidence intervals) of network-scale GPP are shown for a 2621 km^2 watershed under different levels representing the extent of riparian clearing.

Our modeled productivity regimes indicate how the biological properties of river networks respond to changes in network size. In our simulated networks, streambed surface area accumulates faster than drainage area. Therefore, annual, network-scale GPP scales allometrically (exponent > 1) with watershed size, such that river-network GPP increases disproportionately faster than change in drainage area. In the *Stochastic* and *Unproductive rivers* scenarios, mean daily GPP normalized for streambed surface area was relatively invariant with watershed size. In contrast, larger watersheds were more productive on an average areal basis in the *Productive rivers* scenario, resulting in a steeper slope between annual, network-scale GPP and drainage area. We focused our analysis to explore how patterns in network-scale productivity change with watershed size and differences in the spatial arrangement of reach-scale GPP. However, other factors such as network shape and geomorphic structure may shift the accumulation of benthic surface area and, by extension, primary production. For example, network elongation changes the relative proportion of small vs. large rivers and can influence biogeochemical processing at network-scales (Helton et al. 2017). Although the simulations shown here are not a model for any specific real ecosystem, OCNs are most effective for simulating networks in runoff-generating catchments where geomorphology is primarily driven by erosion. These networks are thus not suitable for describing rivers with large floodplains, for example. We therefore expect that differences in river network structure may further expand the variation around the GPP scaling relationships we present here.

Results from simulated networks indicate that river-network productivity is often more persistent throughout the year compared to individual stream reaches. In addition, the confidence interval around a given network-scale productivity regime narrows as river networks increase in size and differences among reaches are averaged out. Network-scale attenuation of the spatiotemporal variability in GPP among individual stream reaches could be important for food webs or metacommunity dynamics (Schindler et al. 2010)—as mobile animals travel through or otherwise "sample" river networks as individuals or populations—or for network-scale nutrient cycling, which may not be limited to the season of peak productivity in any given stream reach.

The fractal nature and geomorphic scaling of river networks means that the number of small streams increases in larger watersheds (Horton 1945), and so their contribution to network-scale GPP is substantial across a range in watershed size. We hypothesize that factors affecting benthic surface area or metabolic activity in small streams, including stream burial (Elmore and Kaushal 2008) or variable patterns of drying and intermittency (Stanley et al. 2004; Datry et al. 2014), will disproportionately affect network-scale productivity. For example, given the importance of light at the scale of individual stream reaches (Bott et al. 2006; Roberts et al. 2007), and the prevalence of small streams in river networks, we expect that variability in the light regime in headwater streams will likely impact both the amount and timing of productivity across river networks. In our riparian clearing scenario, the three disparate model scenarios converged on a similar temporal pattern in GPP as more streams adopted the "summer peak" productivity regime. Of course, unshaded headwaters are not unique to human-altered landscapes, and GPP dynamics in the riparian clearing scenario may also reasonably represent river networks draining prairie, alpine, or desert landscapes. Within and across river networks, predictable seasonality in ecosystem energetic regimes likely influences the identity of the biotic communities that can live there (Tonkin et al. 2017). We therefore suggest that altered watershed land use can shift both the timing and spatial arrangement of productivity at river-network scales, and thus may increase the likelihood for phenological mismatches between aquatic organisms and ecosystem processes (Bernhardt et al. 2018).

Conceptual models of aquatic metabolism have largely described rivers as continua, and rarely as networks (Fisher et al. 2004). We show how concepts of stream metabolism developed at the scale of individual river reaches allow for initial predictions of the primary productivity of entire river networks. The envelope of possible river-network productivity regimes we present here provides greater mechanistic understanding of the factors that influence ecosystem productivity

in real drainage networks. As more spatially extensive river metabolism data sets become available, further research can begin to address how terrestrial biome, hydrologic regime, land use distribution, and the structure and connectivity of river–lake networks shape emergent patterns in productivity across freshwater landscapes.

References

Bernhardt, E. S., and others. 2018. The metabolic regimes of flowing waters. Limnol. Oceanogr. **63**: S99–S118. doi:10.1002/lno.10726.

Bott, T. L., J. T. Brock, C. S. Dunn, R. J. Naimann, R. W. Ovink, and R. C. Peterson. 1985. Benthic community metabolism in four temperate stream systems: An inter-biome comparison and evaluation of the river continuum concept. Hydrobiologia **123**: 3–45. doi:10.1007/BF00006613.

Bott, T. L., J. D. Newbold, and D. B. Arscott. 2006. Ecosystem metabolism in piedmont streams: Reach geomorphology modulates the influence of riparian vegetation. Ecosystems **9**: 398–421. doi:10.1007/s10021-005-0086-6.

Creed, I. F., T. Hwang, B. Lutz, and D. Way. 2015. Climate warming causes intensification of the hydrological cycle, resulting in changes to the vernal and autumnal windows in a northern temperate forest. Hydrol. Process. **29**: 3519–3534. doi:10.1002/hyp.10450.

Csardi, G., and T. Nepusz. 2006. The igraph software package for complex network research. InterJournal, Complex Syst. 1695.

Datry, T., S. T. Larned, and K. Tockner. 2014. Intermittent rivers: A challenge for freshwater ecology. Bioscience **64**: 229–235. doi:10.1093/biosci/bit027.

Elmore, A. J., and S. S. Kaushal. 2008. Disappearing headwaters: Patterns of stream burial due to urbanization. Front. Ecol. Environ. **6**: 308–312. doi:10.1890/070101.

Finlay, J. C. 2011. Stream size and human influences on ecosystem production in river networks. Ecosphere **2**: 87. doi:10.1890/ES11-00071.1.

Fisher, S. G., R. A. Sponseller, and J. B. Heffernan. 2004. Horizons in stream biogeochemistry: Flowpaths to progress. Ecology **85**: 2369–2379. doi:10.1890/03-0244.

Hall, R. O., Jr., and E. R. Hotchkiss. 2017. Stream metabolism. *In* F. R. Hauer and G. A. Lamberti [eds.], *Methods in stream ecology*, v. **2**, p. 219–233. 3rd ed. Academic Press.

Helton, A. M., R. O. Hall, and E. Bertuzzo. 2017. How network structure can affect nitrogen removal by streams. Freshw. Biol. **63**: 128–140. doi:10.1111/fwb.12990.

Horton, R. E. 1945. Erosional development of streams and their drainage basins; hydrophysical approach to quantitative morphology. GSA Bull. **56**: 275.

Julian, J., M. Doyle, and E. Stanley. 2008*a*. Empirical modeling of light availability in rivers. J. Geophys. Res. Biogeosci. **113**, G03022. doi:10.1029/2007JG000601.

Julian, J., E. Stanley, and M. Doyle. 2008*b*. Basin-scale consequences of agricultural land use on benthic light availability and primary production along a sixth-order temperate river. Ecosystems **11**: 1091–1105. doi:10.1007/s10021-008-9181-9.

Leopold, L. B., and T. J. Maddock. 1953. The hydraulic geometry of stream channels and some physiographic implications. Geological Survey Professional Paper, No. 252, U.S. Government Printing Office.

McCluney, K. E., N. L. Poff, M. A. Palmer, J. H. Thorp, G. C. Poole, B. S. Williams, M. R. Williams, and J. S. Baron. 2014. Riverine macrosystems ecology: Sensitivity, resistance, and resilience of whole river basins with human alterations. Front. Ecol. Environ. **12**: 48–58. doi:10.1890/120367.

McTammany, M. E., J. R. Webster, E. F. Benfield, and M. A. Neatrour. 2003. Longitudinal patterns of metabolism in a southern Appalachian river. J. North Am. Benthol. Soc. **22**: 359–370. doi:10.2307/1468267.

Montgomery, D. R. 1999. Process domains and the river continuum. J. Am. Water Resour. Assoc. **35**: 397–410. doi:10.1111/j.1752-1688.1999.tb03598.x.

Poole, G. C. 2002. Fluvial landscape ecology: Addressing uniqueness within the river discontinuum. Freshw. Biol. **47**: 641–660. doi:10.1046/j.1365-2427.2002.00922.x.

R Core Team. 2018, *R: A language and environment for statistical computing*. R Foundation for Statistical Computing.

Rinaldo, A., I. Rodriguez-Iturbe, R. Rigon, R. L. Bras, E. Ijjasz-Vasquez, and A. Marani. 1992. Minimum energy and fractal structures of drainage networks. Water Resour. Res. **28**: 2183–2195. doi:10.1029/92WR00801.

Roberts, B. J., P. J. Mulholland, and W. R. Hill. 2007. Multiple scales of temporal variability in ecosystem metabolism rates: Results from 2 years of continuous monitoring in a forested headwater stream. Ecosystems **10**: 588–606. doi:10.1007/s10021-007-9059-2.

Rodríguez-Castillo, T., E. Estévez, A. M. González-Ferreras, and J. Barquín. 2018. Estimating ecosystem metabolism to entire river networks. Ecosystems **22**: 892–911. doi:10.1007/s10021-018-0311-8.

Rodríguez-Iturbe, I., and A. Rinaldo. 2001, *Fractal river basins: Chance and self-organization*. Cambridge Univ. Press.

Saunders, W. C., N. Bouwes, P. McHugh, and C. E. Jordan. 2018. A network model for primary production highlights linkages between salmonid populations and autochthonous resources. Ecosphere **9**: e02131. doi:10.1002/ecs2.2131.

Savoy, P. 2019. Supporting data for Savoy et al. (2019): Metabolic rhythms in flowing waters: An approach for classifying river productivity regimes, HydroShare. http://www.hydroshare.org/resource/eba152073b4046178d1a2ffe9a897ebe. Dataset accessed 03 June 2019.

Savoy, P., A. P. Appling, J. B. Heffernan, E. G. Stets, J. S. Read, J. W. Harvey, and E. S. Bernhardt. 2019. Metabolic rhythms in flowing waters: An approach for classifying

river productivity regimes. Limnol. Oceanogr. Early view online. doi:10.1002/lno.11154.

Schindler, D. E., R. Hilborn, B. Chasco, C. P. Boatright, T. P. Quinn, L. A. Rogers, and M. S. Webster. 2010. Population diversity and the portfolio effect in an exploited species. Nature **465**: 609–612. doi:10.1038/nature09060.

Stanley, E. H., S. G. Fisher, and J. B. Jones. 2004. Effects of water loss on primary production: A landscape-scale model. Aquat. Sci. **66**: 130–138. doi:10.1007/s00027-003-0646-9.

Tonkin, J. D., M. T. Bogan, N. Bonada, B. Rios-Touma, and D. A. Lytle. 2017. Seasonality and predictability shape temporal species diversity. Ecology **98**: 1201–1216. doi:10.1002/ecy.1761.

Uehlinger, U. 2000. Resistance and resilience of ecosystem metabolism in a floodprone river system. Freshw. Biol. **45**: 319–332. doi:10.1111/j.1365-2427.2000.00620.x.

Uehlinger, U. 2006. Annual cycle and inter-annual variability of gross primary production and ecosystem respiration in a floodprone river during a 15-year period. Freshw. Biol. **51**: 938–950. doi:10.1111/j.1365-2427.2006.01551.x.

Vannote, R., G. Minshall, K. Cummins, J. Sedell, and C. Cushing. 1980. The river continuum concept. Can. J. Fish. Aquat. Sci. **37**: 130–137. doi:10.1139/f80-017.

Acknowledgments

We thank the editors and anonymous reviewers for their comments and suggestions that greatly improved the manuscript. This research is a product of the StreamPULSE project, which was supported by the National Science Foundation (NSF) Macrosystems Biology Program (grant EF-1442451 to AMH, EF-1834679 to ROH, and EF-1442439 to ESB and JBH).

Submitted 05 March 2019
Revised 07 June 2019
Accepted 16 July 2019